ELSEVIER

Journal of Nuclear Materials 244 (1997) 22–28

journal of nuclear materials

Molecular dynamics simulation of low-energy atomic displacement cascades in a simplified nuclear glass

J.M. Delaye [a,*], D. Ghaleb [b]

[a] DTA / DECM / SRMP: Saclay Research Center, Commissariat à l'Energie Atomique (CEA), 91191 Gif-sur-Yvette cedex, France
[b] DCC / DRDD / SCD: Rhône Valley Research Center, Commissariat à l'Energie Atomique (CEA), BP 171, 30207 Bagnols-sur-Cèze cedex, France

Received 9 August 1996; accepted 7 November 1996

Abstract

In a simplified (SiO_2, B_2O_3, Na_2O_3, Al_2O_3, ZrO_2) nuclear glass the authors simulated secondary cascades resulting from the first atoms displaced by a collision with a recoil nucleus. Although the acceleration energies applied to the primary atom were relatively low, the study yielded a number of interesting results, notably concerning a tendency toward diminishing network connectivity, the nature of the atoms most frequently displaced and the mechanisms involved.

1. Introduction

One of the primary sources of irradiation in nuclear glass is α decay of the actinides (U, Pu, Np, Am, Cm) contained within [1]. Recoil nuclei are responsible for most of the atomic displacement cascades generated in the glass [2,3]; we have therefore attempted to apply molecular dynamics to model the atomic displacements induced by the deceleration of a recoil nucleus in a simplified nuclear glass. The path of the recoil nucleus is not specifically represented in this study, but rather the secondary cascades generated by the primary atoms displaced by the collision with the recoil nucleus.

Considering the size of the model ($\sim$ 5000 atoms), the acceleration energies applied to the atom initiating the cascade were limited to between 100 and 800 eV.

2. Cascade modeling principle

A numerical model of a simplified nuclear glass [4] comprising 5 oxides (63.8% SiO_2, 17.0% B_2O_3, 13.4% Na_2O_3, 4.0% Al_2O_3 and 1.8% ZrO_2) was developed using pair potentials modulated by three-body terms for certain components (SiO_2, B_2O_3, Al_2O_3). Born–Mayer–Huggins potentials are applied to each pair of atoms i–j:

$$\phi(r_{ij}) = A_{ij}\exp\left(-\frac{r_{ij}}{\rho_{ij}}\right) + \frac{1}{4\pi\ _0}\frac{q_i q_j}{r_{ij}}, \tag{1}$$

where q_i and q_j are the formal charges of atoms i and j, and A_{ij} and ρ_{ij} are adjustable parameters with values indicated in Table 1. The Coulomb interaction forces for each atom were calculated using the complete Ewald sum method.

Three-body potentials are also used to account for the highly covalent nature of the Si–O and B–O bonds. Each atom triplet j–i–k was characterized by interatomic distances r_{ij}, r_{ik} and angle θ_{jik}, and was assigned a potential energy of the following form [5]:

$$\phi(r_{ij}, r_{ik}, \theta_{jik}) = \lambda_i \exp\left(\frac{\gamma_{ij}}{r_{ij}-r_c} + \frac{\gamma_{ik}}{r_{ik}-r_c}\right)(\cos\theta_{jik} - \cos\theta_0)^2. \tag{2}$$

The adjustable parameters λ_{ij}, γ_{ij}, and γ_{ik} are indicated in Table 2.

Short-range interactions (< 1 Å) liable to occur during the collision sequences are represented by a Ziegler potential [6], which is an experimentally adjusted universal pair potential. Fifth-order polynomial functions were used to

* Corresponding author.

PII S0022-3115(96)00719-2

Table 1
Values of A_{ij} (in 10^{-8} erg). $\rho_{ij} = 0.29$ Å except for O–O interactions ($\rho_{O-O} = 0.35$ Å)

	Si	O	B	Na	Zr	Al
Si	13.4	25.17	5.79	13.81	40.97	15.40
O		5.65	12.19	22.37	76.98	27.78
B			1.94	6.00	16.53	6.35
Na				13.49	42.26	15.64
Zr					125.32	47.11
Al						17.63

Table 2
Values of three-body potential parameters (energies in 10^{-11} erg and distances in Å)

	O–Si–O	Si–O–Si	O–B–O
γ_i	24	1	1920
$\gamma_{ij} = \gamma_{ik}$	2.6	2.0	2.27
θ_0	109.47°	160.0°	109.47°
r_c	3.0	2.6	2.1

ensure continuity of the potential values and their first and second derivatives for the transition from the Ziegler potential to the Born–Mayer–Huggins potentials between 0.9 and 1 Å.

A cascade was simulated by accelerating an oxygen atom at time t_0. The acceleration energy was systematically limited to ensure that the expansion volume resulting from the cascade did not extend outside the simulated system. Introducing a perturbation such as an accelerated atom leads to a series of atomic collisions that considerably increase the kinetic energy of the atoms, and thus the temperature. In order to dissipate the extra agitation from the system, the outer layer of the simulation cell was temperature-regulated: atom movements in the outer layer were regulated to maintain the layer at room temperature.

3. Results

A series of cascades with an incident energy of less than 800 eV was simulated in a 5184 atom glass model. The cascades were described by characterizing the structural changes and by evaluating changes in macroscopic quantities such as the stored energy.

When an atom is pushed away from its equilibrium site with an increasing energy pulse, we observed either that the atom crossed a potential energy barrier (jumped) or that a local reorganization occurred around the initial site of the atom. In the case of a Si atom jump, the migration barrier distribution was relatively wide, ranging from about 20 eV to 50 eV. The minimum observed barrier was 17.5 eV, corresponding to the acceleration of a Si atom toward the center of one face of the tetrahedron surrounding the atom.

The number of displaced atoms was also estimated, after first determining an empirical limit: an atom was considered 'displaced' if the distance between its initial and final positions exceeded 1 Å. The number of displaced atoms versus the energy of the incident particle (Fig. 1) increases with the energy.

Considering the phenomenon in greater detail, it appears that oxygen and sodium were the atoms most frequently displaced. This is consistent with cascades in SiO_2 simulated by Doan [7], who observed a greater abundance of displaced oxygen atoms. Two factors may account for this behavior:

- The cohesive energies of these atoms in the glass network are lower for Na and O than for the network formers.
- The bulk factor also has an important role: Na atoms are surrounded by a large 'free' volume due to the large Na–O first-neighbor distances (~ 2.5 Å), which may favor Na^+ ion displacements. Similarly, oxygen atoms are generally double-bonded to network formers, and are thus more liable to move than the formers themselves, which are surrounded by three or four oxygen atoms forming a cage.

Fig. 2 shows a typical distribution of atomic displacements for O, Na and network formers (Si, B, Al, Zr). The scattering of the distributions may be considered comparable for all the species; no species of atoms is characterized by longer displacement distances than the others.

As shown in Figs. 3 and 4, the number of displacements first rises rapidly to a peak or plateau. The time necessary for the Na atoms to reach the peak or plateau is systematically longer than for the other atoms; sodium atom displacements are slightly delayed (by about 5×10^{-13} s) compared with the other atoms. The atoms forming the network skeleton are displaced first; the Na^+ ions then displace to readjust their position according to the network modifications.

All the displaced atoms at four successive time steps during a cascade are shown in Fig. 5, where it is clear that the Na^+ ions appear after the other atoms, and generally around the periphery of the damage zone. Only 5 sodium

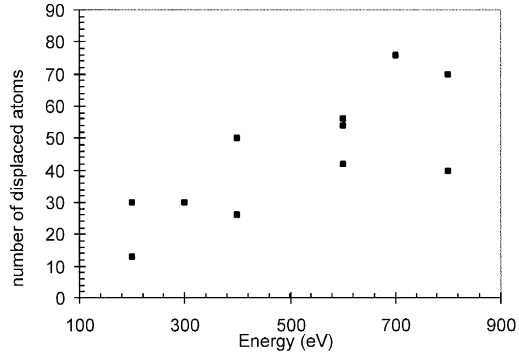

Fig. 1. Number of displaced atoms versus incident energy.

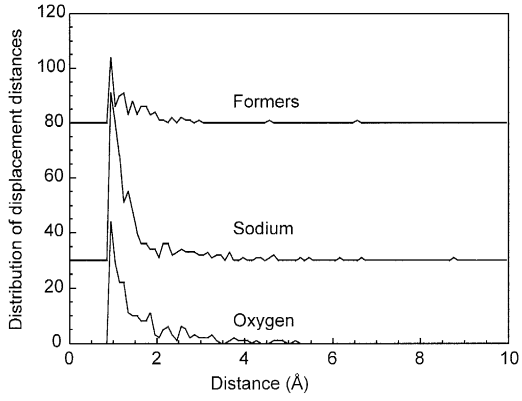

Fig. 2. Typical distribution of displacement distances for various species: O, Na and network formers (Si, B, Al, Zr). The distributions are subjected to large noise considering the small number of displaced atoms.

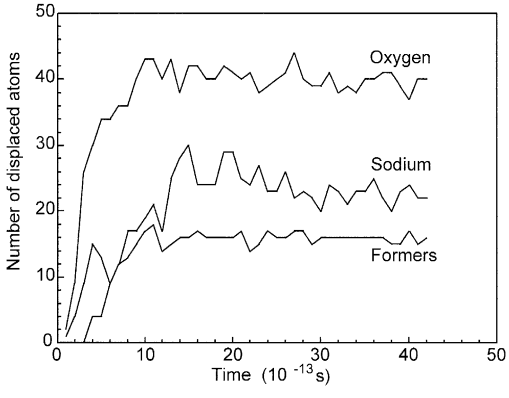

Fig. 3. Typical variation of the number of displacements in time for O, Na and network formers (Si, B, Al, Zr).

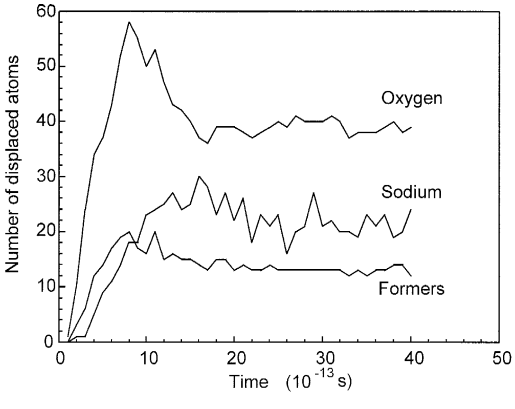

Fig. 4. Typical variation of the number of displacements in time for O, Na and network formers (Si, B, Al, Zr) (same as Fig. 3 for another calculation).

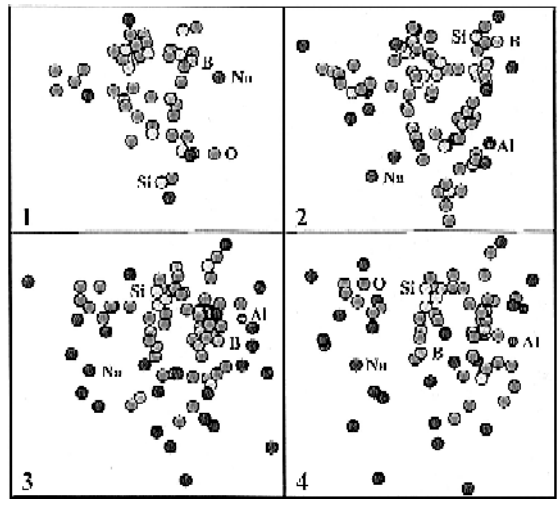

Fig. 5. Positions of displaced atoms for four time steps during a cascade (1: 0.1 ps, 2: 0.16 ps, 3: 0.68 ps, 4: 3.38 ps).

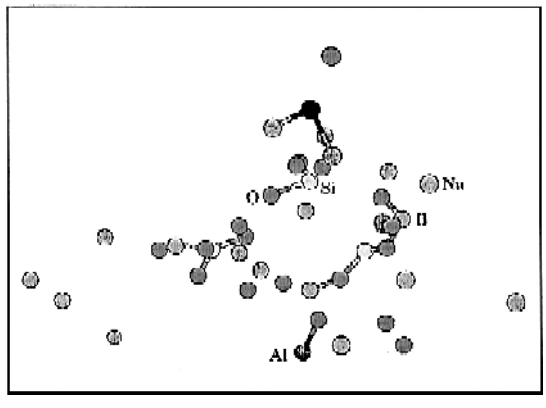

Fig. 6. Displaced atom positions at the end of the cascade after a 5 ps run (1 cm = 1.45 Å).

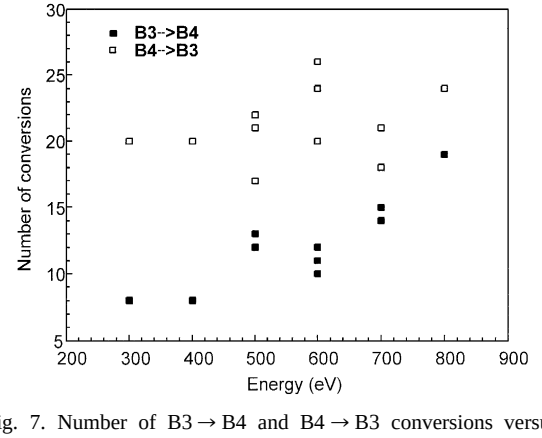

Fig. 7. Number of B3 → B4 and B4 → B3 conversions versus incident energy.

Table 3
Number of $O_3 \leftrightarrow O_2$ and $O_2 \leftrightarrow O_1$ conversions versus cascade incident energy

Incident energy (eV)	$O_3 \rightarrow O_2$	$O_2 \rightarrow O_3$	$O_2 \rightarrow O_1$	$O_1 \rightarrow O_2$
400	26	19	3	2
500	34	29	10	3
500	26	28	7	4
500	27	32	8	4
600	34	30	5	4
600	35	22	9	3
700	32	27	7	4
700	37	34	5	4
800	29	24	5	1
800	35	30	5	3

Table 4
Mean angles around four-coordinate boron atoms. $\langle O–B_4–O \rangle$ is the mean angle calculated for all the boron atoms, $\langle O–B_{3\rightarrow 4}–O \rangle$ is the mean angle calculated for the boron atoms that became four-coordinate during the cascade. Refer to text for the definition of the variation

Incident energy (eV)	$\langle O–B_4–O \rangle$	Mean variation	$\langle O–B_{3\rightarrow 4}–O \rangle$	Mean variation
400	109.27	20.88	109.14	29.87
500	109.27	21.11	109.34	28.97
500	109.29	20.61	109.15	30.85
500	109.28	20.77	109.19	32.25
700	109.27	20.90	109.37	28.04
800	109.28	20.89	109.18	28.82

atoms are visible at step 1, 13 at step 2, 26 at step 3 and 23 at step 4. Fig. 6 shows a damage zone in its final state after a 500 eV cascade. The displaced portions of the network are indeed surrounded by displaced sodium atoms. It is interesting to note that entire portions of the network structure are displaced collectively, rather than one atom at a time; the energy necessary for a collective displacement of a network fragment is certainly lower than the sum of the displacement energies of the constituent atoms.

Some structural changes were revealed in the damaged glass volume. The most striking of these are the local order modifications around boron and oxygen atoms.

The coordination number of some boron atoms changes from 4 to 3 or vice versa during a displacement cascade. When the number of such conversions is plotted versus the incident energy of the cascade (Fig. 7) the number of four-coordinate boron (B4) to three-coordinate boron (B3) conversions is systematically higher than the number of B3 to B4 conversions, i.e., the total number of three-coordinate boron atoms increases during a displacement cascade.

The other significant structural modification observed involved oxygen atoms. In vitreous models the oxygen coordination numbers are 2 (90% of the O atoms), 3 (5%) and 1 (5%) [8]. During the cascade, the mean coordination number of the oxygen atoms diminishes, and the number of O1 (non-bridging oxygen) atoms increases. Table 3 indicates the number of O3 → O2 and O2 → O1 conversions and the reciprocal conversions versus the incident energy. O2 ↔ O3 conversions are more numerous than O2 ↔ O1 conversions, and the number of conversions appears to be independent of the incident energy.

Fig. 8 includes a sequence of six images illustrating a typical conversion of four-coordinate boron to three-coordinate boron. Before the collision (image 1) the boron atom at the center of the image has a coordination number of 4. Image 2 shows the rupture of the 4 bonds around the B atom immediately after the passage of the accelerated atom. Image 3 shows the reconstructed bonds around the central boron atom; only four of the initial bonds are reformed, and this condition persists until the final configuration (image 6). Along with this change in the boron

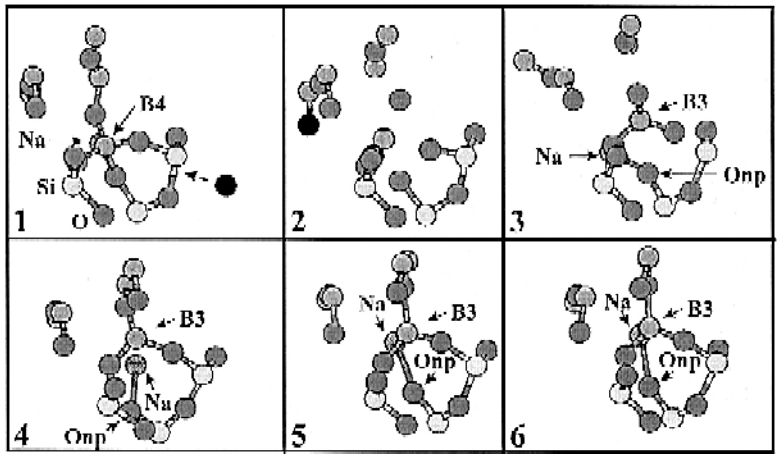

Fig. 8. Example of conversion of 4-coordinate boron (B4) to 3-coordinate boron (B3) and formation of a nonbridging oxygen atom (O_{nb}).

coordination number, a bridging oxygen atom can be seen to become non-bridging. The oxygen atom initially bonded to the boron atom is bonded to a silicon atom and a sodium atom at the end of the simulation, and is now non-bridging. Closer examination of the B4 → B3 conversions shows that they are often related to O3 → O2 or O2 → O1 conversions.

Very few structural modifications occur around Si atoms and, in particular, only a few Si4 atoms are converted to Si3. The formation of three-coordinate silicon (which, from a structural standpoint, may be considered as E′ centers, i.e., an oxygen vacancy near a silicon atom) is made difficult by the stability of the silicon atom sites. Similarly, few modifications are observed around aluminum atoms.

The observed changes affecting the local angles in the structure correspond to increasing disorder, notably with regard to the increasingly wide distribution of local angles around the boron atoms. For all the B4 → B3 and B3 → B4 conversions, we measured the mean angles around the B4 atoms and the maximum variation among the angles for each tetrahedron (Table 4). The 'variation' is defined as the difference between the maximum and minimum angles around each boron atom. As shown in Table 4, the mean variation of the angles around the B4 atoms created during the cascades is greater than for all the B4 atoms; the deformation of the B4 tetrahedrons resulting from the conversions is greater than the mean deformation of all the B4 tetrahedrons. Conversely, the increasing angular disorder observed around the B3 atoms created during the displacement cascades (Table 5) is less significant.

We tested a method for estimating the volume of a displacement cascade. The method involves determining the center of gravity of the displaced atoms, and plotting the distribution of the distances between the displaced atoms and the center of gravity. The extent of the distribution provides a rough approximation of the diameter of the damaged volume. Fig. 9 shows a typical distribution for a 700 eV cascade. The shift toward increasing distances around the sodium atoms confirms that displaced Na^+ ions tend to be found around the periphery of the damage zone. Despite the extensive scattering of the points, it may be seen that the mean distance between the displaced atoms and the center of gravity increases with the incident energy of the cascade (Fig. 10).

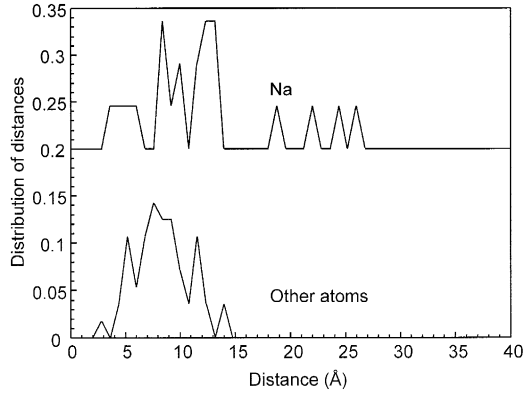

Fig. 9. Distribution of distances between displaced atoms and their center of gravity. Two separate distributions were calculated: Na atoms alone, and all other atoms together.

Although in most cases the total potential energy increases after each cascade, the stored energy following the cascades is relatively low (Fig. 11). The points were too scattered to demonstrate any clear correlation between the stored energy and the incident energy. Given the model glass density of 2.5 g cm^{-3}, a stored energy of 10^{-10} erg in a 5184 atom system corresponds to about 70 J g^{-1}. Experimental findings [1] have shown that the stored energy in doped nuclear glasses does not exceed about 150 J g^{-1}. The number of displacements per atom (dpa) in these simulations was about 0.02 (i.e., about a hundred atoms displaced out of 5184). However the validity of the com-

Table 5
Mean angles around three-coordinate boron atoms. $\langle O–B_3–O\rangle$ is the mean angle calculated for all the boron atoms, $\langle O–B_{4\to3}–O\rangle$ is the mean angle calculated for the boron atoms that became three-coordinate during the cascade. Refer to text for the definition of the variation

Incident energy (eV)	$<O–B_3–O>$	Mean variation	$<O–B_{4\to3}–O>$	Mean variation
400	114.66	6.69	113.72	8.56
500	114.83	7.90	113.93	7.89
500	114.67	6.73	114.48	9.95
500	114.65	6.61	113.86	8.88
700	114.71	7.12	113.22	9.05
800	114.9	6.52	114.46	10.63

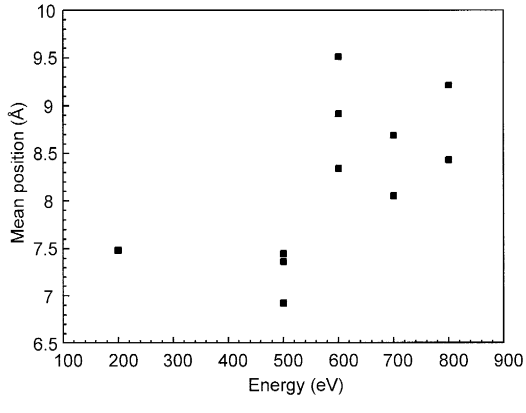

Fig. 10. Mean position of total distribution (for all atoms) of distances between displaced atoms and their center of gravity versus incident energy.

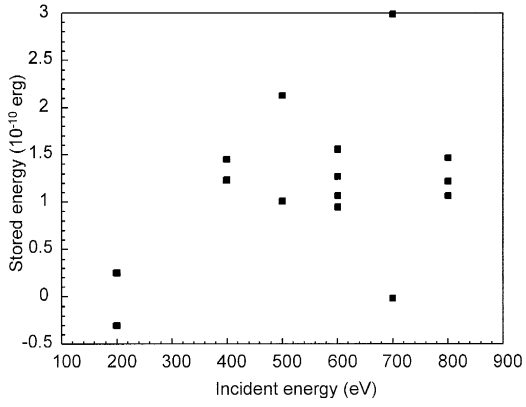

Fig. 11. Stored energy in the system versus incident energy.

parison may be limited since the cohesive energies are not realistically represented by Born–Mayer–Huggins potentials when formal ion charges are used.

4. Discussion

We want first to address the problem of the quench of the external layer of the simulation cell and its consequence on the evolution of the cascade. We have performed simulations at 700 eV with and without controlling the external layer. Two cases have been studied. The first one shows practically no differences between the two simulations: there are 93 displaced atoms when the temperature of the external layer is controlled and 87 displaced atoms when the temperature of the external layer is free.

The second calculation presents a larger difference: there are 84 displaced atoms when the external layer is not controlled and only 58 when the external layer is controlled. This larger difference is due to the longer distance covered by the PKA. When the trajectory of the PKA is short, as in the first case, the volume of the displacement cascade is contained inside the simulation cell, but on the contrary, when the trajectory of the PKA is longer, as in the second case, the displacement cascade extends beyond the external layer when no control is applied. So in the first case, the control of the external layer has a weak effect on the result, but this is not true in the second case.

It means that for the larger energies, the control of the external layer tends to limit the number of displaced atoms, and consequently, the volume of the damaged zone. The distribution of the number of displaced atoms on Fig. 1 is probably enhanced because of this phenomenon.

The results of these simulations raise several questions that warrant further investigation.

The first point concerns the influence of three-body potential terms on the final result, and notably on the variation in the boron coordination number. A relatively high tetrahedral constraint was required on the O–B–O angles to fit the percentage of four-coordinate boron with the experimental findings [4]. What is the effect of this strong three-body term on the number of B4 → B3 conversions? The best way to answer this question is to simulate displacement cascades in a system with no three-body terms around the boron atoms. The slope of Fig. 1 may be extrapolated to estimate the number of displaced atoms at about 10 000 per disintegration, based on the mean energy of a recoil nucleus. This exceeds the generally accepted values of 1500 to 2000 atoms [9,10] supplied by binary collision models based on migration thresholds for each atom. Various explanations may be advanced to account for this difference:

– First, a plateau may be reached at higher energies, or the slope of the curve may diminish. Nevertheless, no published results have been obtained in metallic crystalline structures that reveal any saturation of the number of displaced atoms versus the incident energy.

– Second, and more plausibly, phenomena involving collective displacement of entire portions of the network are not correctly taken into account in binary collision models.

Concerning the effect of the glass composition on the cascade morphology, we have already noted that the cascade expansion volume was bordered by Na atoms that readjusted their positions in response to the change in the Coulomb field resulting from the structural modifications of the cascade. Does sodium therefore have a passive role in the expansion (i.e., the Na atoms relocate themselves according to the structural modifications) or an active role (i.e., the Na atoms interact directly with the cascading expansion and terminate its propagation)? The second hypothesis raises further questions: Does the volume of the damage zone increase when the alkali metal concentration diminishes? Does the path length of the initial particle depend on the Na_2O concentration? The results presented here were obtained by simulating ballistic collisions among atoms, without allowing for electron losses. An unanswered question at this time concerns the possible effects of electron losses on the morphology of the displacement cascade (about 10–20% of the incident particle energy is dissipated in the form of electron losses [2,3]). The modification of the charges by ionization could modify the interaction forces within the cascade, and thus also affect the number of displaced atoms, the number of defects created, and the reorganization at the end of the cascade. Conventional molecular dynamics methods that do not represent electrons are currently unable to answer this question.

A final point is the absence of peroxide defects [11] in the simulations; this type of defect is unstable with the potentials used here. In the coming months we shall attempt to find a solution for stabilizing such defects, and determine whether the number and arrangement of the defects could constitute the initial stages in the formation of O_2 bubbles.

This study highlights some of the limits of the potentials currently used, which are reliable for overall structural modeling but less so from an energy standpoint. The overall pattern of an irradiation cascade as perceived from this study (collective displacements of network portions; peripheral location of displaced sodium atoms; number of displaced atoms proportional to the incident energy) is a reliable model directly based on the inherent nature of the amorphous network comprising formers and modifiers. Conversely, the details of structural changes — notably changes in the coordination number, which certainly depend on the potential used — should be confirmed by using potentials that more closely approximate the actual energies.

5. Conclusions

Although the acceleration energies applied to the initial atom were relatively low (100–800 eV) this molecular dynamics investigation of displacement cascades in a simplified nuclear glass (SiO_2, B_2O_3, Na_2O_3, Al_2O_3, ZrO_2) provided interesting data at atomic scale:

– The number of displaced atoms increases with the incident energy.

– Oxygen and sodium are the most frequently displaced atoms.

– Sodium atom displacements are slightly delayed with respect to the other atoms.

– Most of the displaced Na atoms are found around the periphery of the cascade.

– No species of atoms is displaced over longer distances than the others.

– Collective atomic displacements involving entire portions of the network were identified.

– A tendency was also observed for the coordination numbers of boron (B4 → B3) and oxygen (bridging oxygen → non-bridging oxygen) to diminish, thereby diminishing the network connectivity.

Acknowledgements

The authors are grateful to CEA(DCC/DRDD/SCD) and COGEMA for the financial support of this study. Dr N. Van Doan kindly provided the original program for development of the simulations and, together with Dr Y. Limoge, provided valuable insights after a critical reading of this paper.

References

[1] W.J. Weber, Nucl. Instrum. Methods Phys. Rev. B32 (1988) 471.
[2] M.T. Robinson, J. Nucl. Mater. 216 (1994) 1.
[3] L.W. Hobbs, F.N. Clinard, S.J. Zinkle and R.C. Ewing, J. Nucl. Mater. 216 (1994) 291.
[4] J.M. Delaye and D. Ghaleb, Mater. Sci. Eng. B37 (1996) 232.
[5] B.P. Feuston and S.H. Garofalini, J. Chem. Phys. 89 (1988) 5818.
[6] D.J. O'Connor and J.P. Biersack, Nucl. Instrum. Methods Phys. Rev. B15 (1986) 14.
[7] N.V. Doan, Philos. Mag. A49 (1984) 683.
[8] S.H. Garofalini, J. Non-Cryst. Solids 63 (1984) 337.
[9] W. Lutze and R.C. Ewing, Silicate Glasses in Radioactive Waste Forms for the Future (North-Holland, Amsterdam, 1988) p. 66.
[10] W.J. Weber and F.P. Roberts, Nucl. Technol. 60 (1983) 178.
[11] Y. Adda, A. Barbu, G. Brebec, N.V. Doan, R. Gupta, Y. Limoge, B. Perraillon, P. Regnier and Y. Serruys, Ann. Chim. Fr. 10 (1985) 499.